STRUCTURES AND FUNCTIONS OF THIN METAL LAYERS ON SEMICONDUCTOR ELECTRODES*

YOSHIHIRO NAKATO and HIROSHI TSUBOMURA

Laboratory for Chemical Conversion of Solar Energy, Faculty of Engineering Science, Osaka University, Toyonaka, Osaka 560 (Japan)

Summary

Metal-coated semiconductor electrodes such as Au/n-TiO_2 and Au/n-GaP show photovoltaic effects that cannot be explained by the conventional potential barrier model for metal–semiconductor contact. From experimental and theoretical investigations it has been concluded that the microscopically discontinuous structure of the metal layer is responsible for the anomalous photovoltaic effect. Several theoretical conclusions which are interesting from the point of view of solar energy conversion are derived.

(1) Metal-coated semiconductor electrodes in electrolyte solutions generate high photovoltages at the metal–semiconductor interface in cases where the metal layer forms islands approximately 5 nm in diameter and separated by more than 20 nm from each other provided that the potential of the electrode is controlled so as to give band bending in the metal-free part of the surface. The maximum photovoltage can increase up to the equivalent of the band gap of the semiconductor in ideal cases.

(2) The metal–semiconductor contact becomes ohmic when the potential of the electrode approaches the flat-band potential for the bare electrode in cases where the metal layer either has cracks or forms islands with gaps wider than 20 nm, say.

Changes in the barrier height at the metal–semiconductor interface are not assumed in the theory, which can be applied to any metal–semiconductor pair. The conclusions provide a theoretical basis for the explanation of the mechanisms of interesting properties of metal-coated semiconductor photoelectrodes and photocatalysts, such as enhanced hydrogen photoevolution on platinum-coated p-type semiconductor electrodes or on platinum-coated semiconductor particles in solution.

1. Introduction

Extensive studies have been made on semiconductor photoelectrochemical cells with a view to solar energy conversion. We reported some years ago

*Paper presented at the Fifth International Conference on Photochemical Conversion and Storage of Solar Energy, Osaka, Japan, August 26 - 31, 1984.

0047-2670/85/$3.30

that thin noble metal coating effectively prevents the corrosion of n-type silicon and other semiconductor electrodes [1, 2]. The thin metal coating also catalysed photoelectrode reactions, *e.g.* the photoevolution of hydrogen on p-type silicon and GaP electrodes [3]. These functions of the thin metal layers are quite interesting, and the metal coating has recently been widely used not only for photoelectrodes [4 - 9] but also for suspended powder photocatalysts [10 - 13].

The main difficulty with metal-coated semiconductor photoelectrodes arises from the fact that the photovoltages generated are low [1, 2] owing to the low potential barriers formed at the metal–semiconductor contacts. In order to achieve efficient chemical conversion of solar energy, we have investigated silicon electrodes containing p–n junctions and coated with a platinum layer 1 - 3 nm thick. Electrochemical cells with electrodes of this type photoelectrolysed hydrogen iodide into hydrogen and iodine (or I_3^- ions) with a high solar-to-chemical conversion efficiency of 8.2% under air mass 1 light without external bias [14, 15]. The photocurrent at the maximum power point was maintained by continuous illumination over 4700 h [16].

We have also reported that some gold-coated n-GaP electrodes showed photovoltages much higher than those expected from the barrier height at the Au/n-GaP contact in the dark [2]. Recently, a similar interesting photovoltaic effect has been confirmed for gold- or palladium-coated n-TiO_2 electrodes by direct measurement of the potential of the metal layer [17, 18]. These results cannot be explained using the conventional potential barrier model in which the barrier height is regarded as constant irrespective of whether the contact is in the dark or under illumination. In the present paper we shall discuss the mechanism of the above photovoltaic effect.

2. Brief review of our reported results

As reported in our previous paper [17], gold-coated n-TiO_2 electrodes in aqueous electrolyte solutions give photocurrent–potential curves which are nearly the same as those for bare n-TiO_2 electrodes, indicating that the effective conduction band edge for the Au/n-TiO_2 electrode can be regarded as nearly the same as that for the bare n-TiO_2 electrode. Let us denote the potential of n-TiO_2 in the Au/n-TiO_2 electrode by U(n-TiO_2), the flat-band potential for the bare n-TiO_2 electrode by U_{fb}(n-TiO_2) and the potential of the gold layer by U(Au). Then, if the Au/n-TiO_2 electrode is illuminated in an electrolyte solution and U(n-TiO_2) is maintained a little more positive than U_{fb}(n-TiO_2) using a potentiostat, U(Au) shifts downwards to the water oxidation potential, *e.g.* from about +0.1 V (measured with respect to a saturated calomel electrode (SCE)) in the dark to +1.35 V (SCE) under illumination in a solution of pH 7.0 [17]. These results imply that the height of the potential barrier at the Au/n-TiO_2 contact is increased by illumination, which favours solar energy conversion (Fig. 1(a)) [17].

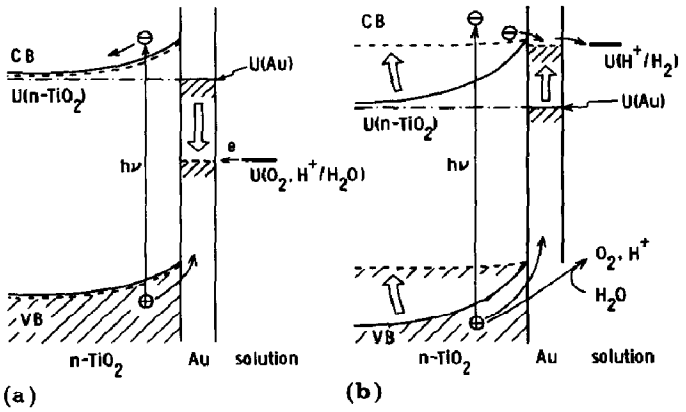

Fig. 1. Energy band models illustrating the photovoltaic effects observed at a gold-coated n-TiO_2 electrode in an aqueous electrolyte solution (a) with and (b) without a potentiostat to control the potential U(n-TiO_2): ——, energy levels in the dark; – – –, energy levels under illumination. The Fermi level E_F is related to the potential U by the equation $E_F = -eU$ + constant. (CB, conduction band; VB, valence band.)

When the gold-coated n-TiO_2 electrode is simply immersed in a deaerated electrolyte solution under no external potential control, U(n-TiO_2) and U(Au) are 0.4 - 0.6 V more positive than U_{fb}(n-TiO_2) in the dark. Both U(n-TiO_2) and U(Au) shift towards U_{fb}(n-TiO_2) under illumination; U(n-TiO_2) moves rapidly and U(Au) rather slowly (Fig. 1(b)) [18]. The Au/n-TiO_2 contact then becomes ohmic or nearly ohmic under illumination. In cases where oxygen is dissolved in the solution, U(TiO_2) shifts in a similar way to before but U(Au) shifts only to the oxygen reduction potential [18].

The onset potentials for hydrogen evolution photocurrents at p-Si and p-GaP electrodes are much more negative than U_{fb} for these electrodes, probably because of the formation of surface states and/or the low catalytic activity of the semiconductor surfaces. The onset potentials are shifted considerably to the positive by the electrochemical deposition of platinum or palladium, while the U_{fb} values themselves remain unchanged (Fig. 2) [3, 15]. Similar interesting results were later reported for p-Si, p-WSe_2 and p-InP by other workers [6 - 9]. In contrast, the p-Si and p-GaP electrodes coated with platinum or palladium by vacuum evaporation show high dark currents, indicating that the metal–semiconductor contacts are nearly ohmic in this case.

3. Present results

For further clarification of the photovoltaic behaviour of metal-coated semiconductor electrodes in aqueous solutions the open-circuit photovoltage V_{oc} between the semiconductor and the metal in a photoelectrochemical cell was measured as a function of the controlled potential U(M) (SCE) of the metal (Fig. 3). The semiconductors used were single-crystal wafers of n-Si

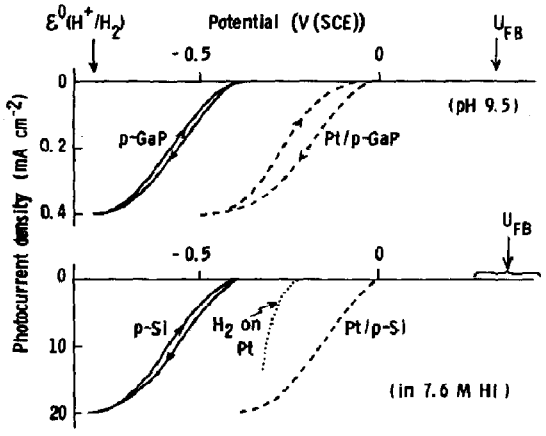

Fig. 2. Hydrogen evolution photocurrent density *vs.* potential curves for p-Si and p-GaP electrodes compared with those for the same electrodes coated with platinum electrochemically.

($N_D \approx 1.0 \times 10^{16}$ cm^{-3}), n-GaP ($N_D \approx (2 - 3) \times 10^{17}$ cm^{-3}) and n-TiO_2 (dark blue coloured). The metals were deposited by vacuum evaporation, the average thickness ranging from 3 to 5 nm. The V_{oc} values for Pt/n-Si and Pt/n-GaP were independent of U(M), as expected from the conventional potential barrier model, while V_{oc} for Au/n-TiO_2 changed linearly with U(M) (Fig. 4). This last result is in harmony with our previous results [17, 18]. The value of V_{oc} for Au/n-GaP changed linearly in the negative U(M) region and became constant in the positive U(M) region. The scanning electron micrographs of the gold layers on n-GaP and n-TiO_2 showed many cracks 10 - 20 nm wide and 40 - 100 nm long, while those of the platinum layers on n-GaP and n-Si had an apparently continuous feature (Fig. 5). These results suggest that the discontinuous contact of the metal layer is responsible for the anomalous photovoltaic effect.

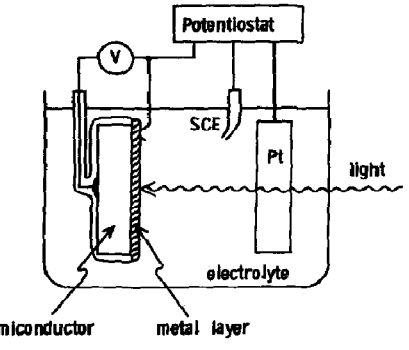

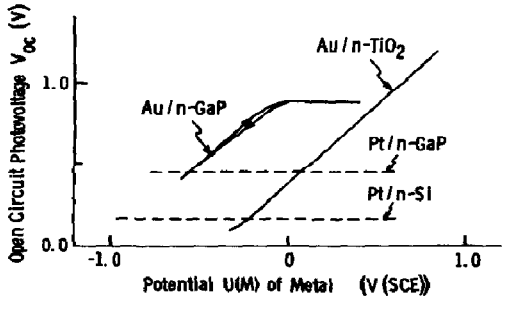

Fig. 3. An experimental set-up for measuring V_{oc} as a function of the potential U(M) (SCE) of the metal layer.

Fig. 4. V_{oc} *vs.* U(M) relationships for metal-coated semiconductor electrodes in an aqueous electrolyte solution of pH 6.8.

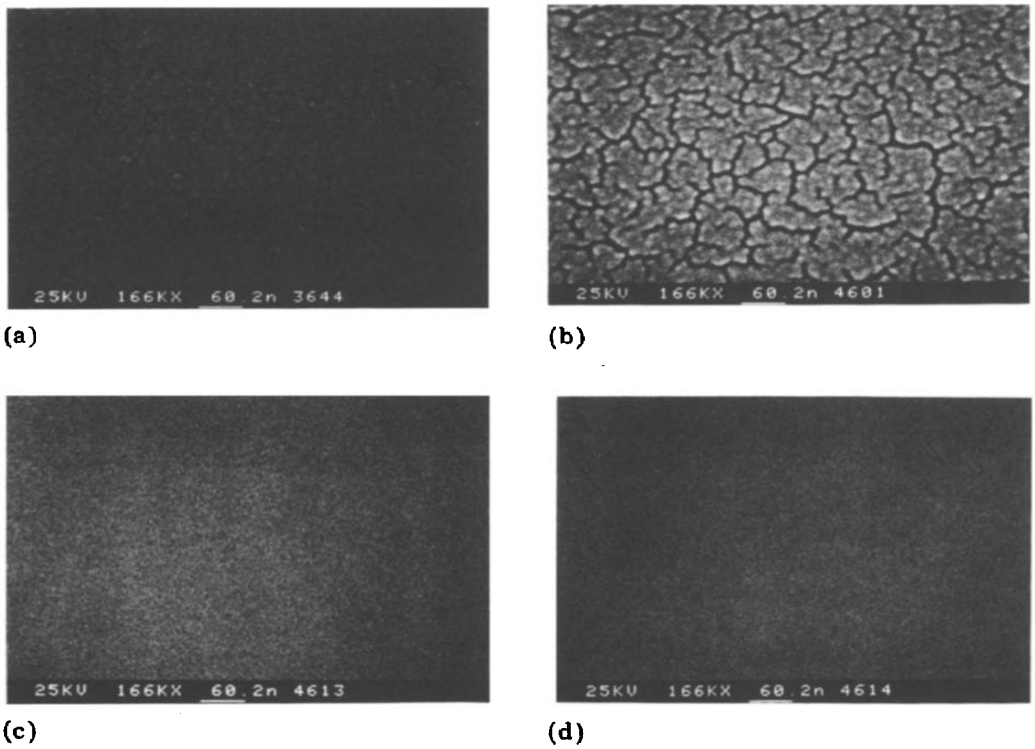

(a) (b)

(c) (d)

Fig. 5. Scanning electron micrographs of gold- or platinum-coated n-GaP single-crystal wafers compared with those of a bare n-GaP wafer and a gold-coated n-TiO_2 wafer: (a) 5 nm of gold on GaP; (b) 3 nm of gold on TiO_2; (c) 3 nm of platinum on GaP; (d) GaP (reference).

The behaviour of the metal-coated electrode, as described above, was changed by changing the coating method, *e.g.* an n-GaP electrode coated with platinum by electrochemical deposition showed an inflected V_{oc} *versus* U(M) curve similar to that for Au/n-GaP in Fig. 4.

4. Theory

The discontinuous metal layers can be classified into five typical cases as shown schematically in Fig. 6. The semiconductor is assumed to be n type, though similar conclusions can also be obtained for p-type semiconductors. In case 1, both the metal and the gap areas are 20 - 100 nm wide. The conduction band edge E_c(S) at the semiconductor–solution interface is determined by the electron affinity of the semiconductor, an ion adsorption equilibrium at the interface etc., while that at the semiconductor–metal interface, E_c(M), is determined by the barrier height $e\phi_B$ at the metal–semiconductor contact and the Fermi level E_F(M) of the metal. Accordingly, the surface band edges of the semiconductor should be modulated as illustrated schematically in Fig. 7. E_c(M) is lower than E_c(S) when E_F(M) is low

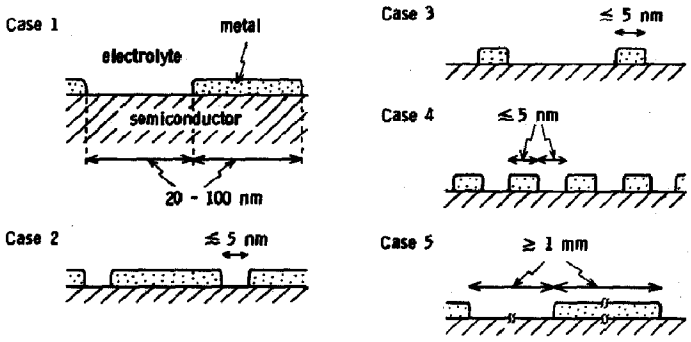

Fig. 6. Schematic diagrams of the discontinuous metal layers.

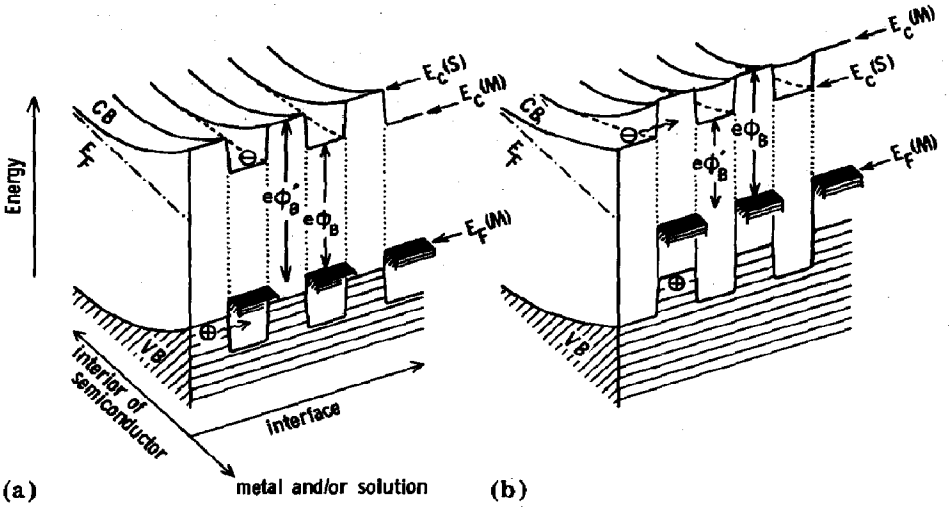

Fig. 7. Schematic diagrams of the modulated potential barriers expected for a metal-coated n-type semiconductor electrode (shown in Fig. 6, case 1) coated discontinuously with metal (the barrier height $e\phi_B$ is taken to be constant, irrespective of E_F(M)): CB, conduction band; VB, valence band.

(Fig. 7(a)), while E_c(M) becomes higher than E_c(S) when E_F(M) is shifted upwards, *i.e.* when U(M) is scanned to the negative (Fig. 7(b)).

The band energies in the space charge region of the semiconductor should also be modulated (Fig. 7). The profile of the modulated bands depends not only on the widths of the metal and gap areas but also on the donor density N_D of the semiconductor, the difference between E_c(S) and E_c(M) etc. The details will be reported elsewhere. It can be shown that substantial band modulation is present in the space charge region in case 1 when N_D is higher than 10^{17} cm^{-3}, say.

It should be noted that the modulation of the bands causes quantization of the energies of the electrons in the conduction band or the holes in the valence band near the interface. A simple calculation using a one-dimensional potential well shows that the zero-point energy is negligibly small when the potential well is wider than 10 nm, even if the effective mass

of the electrons or holes is assumed to be one-tenth of the mass of an electron at rest. We can therefore assume that the lowest energy of the conduction band electrons at the interface lies at the bottom of the modulated conduction band and that the lowest energy of the holes lies at the top of the modulated valence band, as shown by ⊖ and ⊕ in Figs. 7(a) and 7(b). It should be noted also that the electrons or holes which come to the semiconductor–solution interface can enter the metal via quantum mechanical penetration through the potential wall formed by band modulation, as indicated by an arrow in Fig. 7(a) for a hole and in Fig. 7(b) for an electron.

On the basis of the above considerations, it can be concluded that the open-circuit photovoltage V_{oc} between the semiconductor and the metal is determined by

$$e\phi_B = E_c(M) - E_F(M)$$

for the case shown in Fig. 7(a), while V_{oc} is determined by

$$e\phi_B' = E_c(S) - E_F(M)$$

for the case shown in Fig. 7(b). ϕ_B and hence V_{oc} are independent of $E_F(M)$ in the former case, while ϕ_B' and V_{oc} decrease linearly with the upward shift of $E_F(M)$ in the latter case. This explains well the V_{oc} *versus* $U(M)$ relationship for the Au/n-GaP electrode in Fig. 4. In conclusion, the maximum value of V_{oc} is limited by ϕ_B, and the metal–semiconductor contact can become ohmic in case 1.

In Fig. 6, case 2, the gap areas are much narrower, *e.g.* less than 5 nm. It can be assumed that a similar modulation of the surface band edges exists. However, the gaps are so narrow that the band modulation rapidly decreases toward the interior of the semiconductor (the band bending inside the semiconductor is mainly governed by the metal–semiconductor contact). The potential well near the interface is also so narrow that the zero-point energy may be large. Consequently, the energies of the electrons or holes at the semiconductor surface can in this case be regarded as nearly the same as those for an electrode coated with a continuous metal layer. This implies that the electrode in this case behaves as if it were coated with a continuous metal layer and that V_{oc} is determined by the barrier height $e\phi_B$, irrespective of $E_F(M)$.

In case 3 the metal–semiconductor contacts are very narrow. By the same reasoning as above, the energies of the electrons or holes at the semiconductor surface should be nearly the same as those for the electrode with no metal. Therefore V_{oc} in this case is determined by the barrier height $e\phi_B'$ for a wide range of $E_F(M)$. Since $e\phi_B'$ can increase up to the band gap value E_g when $E_F(M)$ is shifted downwards, V_{oc} can become very high, irrespective of the "intrinsic" barrier height $e\phi_B$. It should also be noted that the metal–semiconductor contact in case 3 can become ohmic, as in case 1 (Fig. 7(b)).

In case 4, both the metal and the gap areas are very narrow. In this case the energy of the conduction band edge at the semiconductor surface should be an average value between $E_c(S)$ and $E_c(M)$, and V_{oc} should change with

E_F(M) more gradually than in case 3. Case 5 represents a metal coating which is discontinuous on a macroscopic scale, *i.e.* both the metal and the gap areas are much wider than the diffusion length of the minority carriers. The electrode in such a case behaves like a mixture of the metal-coated electrode and the bare electrode.

5. Discussion

It has been shown in Section 4 that various photovoltaic effects can arise from structural changes in the deposited metal layers and that these effects can be explained without assuming any changes in the intrinsic barrier height $e\phi_B$ at the metal–semiconductor contact. As mentioned before, the inflected V_{oc} *versus* U(M) curve for the Au/n-GaP electrode (Fig. 4) can be explained well using the model shown in Fig. 7. The fact that the V_{oc} *versus* U(M) relationship is linear for the Au/n-TiO_2 electrode suggests that V_{oc} for this case is determined by the barrier height $e\phi_B'$ for a wide range of U(M). The scanning electron micrograph of a gold layer on TiO_2 shows cracks larger than those of a gold layer on n-GaP (Fig. 5). The above result for the Au/n-TiO_2 electrode may be explained if it is assumed that the actual area of contact between the gold and the n-TiO_2 is much narrower than it appears from the micrograph because of poor adhesion between gold and n-TiO_2 and that the structure of the electrode is therefore classified as Fig. 6, case 3.

The anomalous photovoltaic effect depicted in Fig. 1(a) can now be explained as follows: V_{oc} for the Au/n-TiO_2 electrode is determined by $e\phi_B'$, as mentioned above; in other words, the "effective" conduction band edge for the Au/n-TiO_2 electrode is determined by E_c(S) and is nearly equal to that for a bare n-TiO_2 electrode. When the Au/n-TiO_2 electrode is illuminated in the presence of band bending, *i.e.* with U(n-TiO_2) maintained a little more positive than U_{fb}(n-TiO_2), the photogenerated holes arriving at the surface enter the gold layer and shift U(Au) downwards. The shift in U(Au) does not affect the band bending determined by E_c(S) and U(n-TiO_2). Under continued illumination, U(Au) is shifted until it reaches the water oxidation potential.

It is important to emphasize the fact that in the above-mentioned case the potential of the metal layer can shift without affecting the effective surface band edges of the semiconductor and therefore that the metal layer can act as a catalyst for the electrode reaction of the photogenerated minority carriers without changing the energy relationship between the semiconductor and the solution. This mechanism should take place in general for any semiconductor–metal pair if the metal layer is of the structure depicted in Fig. 6, case 3. The mechanism is important for semiconductor electrodes coated with layers of catalyst as is necessary for the promotion of the desired photoelectrode reactions. The considerable enhancement of hydrogen photoevolution at p-type silicon and GaP electrodes by the electrochemical deposition of platinum or palladium (Fig. 2) is interesting in this respect.

Experimental results described previously indicate that deposited metals act as catalysts for hydrogen photoevolution without changing the surface band energies of the semiconductors, exactly as noted above. This can be explained if it is assumed that a small amount of metal, deposited electrochemically, forms tiny islands, as shown in Fig. 6, case 3, and that the effective barrier height is determined by

$$e\phi_B' = E_F(M) - E_v(S)$$

where $E_v(S)$ refers to the valence band edge at the semiconductor–solution interface. $E_F(M)$, *i.e.* $U(M)$, can be shifted upwards to the hydrogen evolution potential by photogenerated electrons coming to the metal under illumination, without affecting the surface band energies. The enhanced hydrogen photoevolution which has been reported on Pt/p-WSe_2 [6] and Rh/p-InP [8] electrodes may be explained in the same way as above.

The phenomenon shown in Fig. 1(b) can be explained as follows. When the Au/n-TiO_2 electrode is illuminated under no external potential control, the photogenerated electrons and holes are separated by band bending. The electrons move into the bulk and are accumulated there. The holes either enter the gold layer or react directly with the solution through the cracks in the gold layer. With continued illumination, U(n-TiO_2) shifts upwards and the band bending diminishes, and finally the electrons in the conduction band spill into the gold layer by electron tunnelling as indicated by $\ominus$ and the arrow in Fig. 7(b). The number of electrons which enter the gold layer is larger than that of holes in a stationary state under illumination because some of the photogenerated holes react with the solution at the semiconductor–solution interface, as mentioned above. (It is tacitly assumed here that the overall rate of reaction of the conduction band electrons at the semiconductor–solution interface under illumination is lower than that of the valence band holes. In cases where the rate of the former reaction is higher than that of the latter, the number of holes entering the metal must be larger than the number of electrons and the potential of the metal must shift towards the positive (*cf.* ref. 18).) Accordingly, the gold layer is negatively charged and U(Au) shifts upwards until the Au/n-TiO_2 contact becomes ohmic (Fig. 1(b)). Since U_{fb}(n-TiO_2) is at nearly the same level as the hydrogen evolution potential, U(Au) shifts to a potential very close to it, and hydrogen may be evolved at the gold surface. In cases where oxygen is dissolved in the solution, U(Au) shifts only to the oxygen reduction potential. The above-mentioned spilling of electrons from the semiconductor to the metal must occur generally if the metal layer takes the structure of Fig. 6, cases 1 or 3, irrespective of the presence of the potential barrier at the metal–semiconductor interface. The mechanism of Fig. 1(b) therefore gives the theoretical basis for the reaction mechanism at metallized powder photocatalysts.

Yamamoto *et al.* found that the current–potential curves for junctions between platinum, palladium or gold and n-TiO_2 in air were shifted by adding hydrogen to the ambient and showed that this was due to the

decrease in the work function of the metal, which is caused by the removal of the surface oxide layer by reaction with hydrogen [19]. Heller *et al.* recently reported similar results for various junctions between platinum, rhodium or ruthenium and n-TiO_2, n-$SrTiO_3$, n-CdS or p-InP and concluded, in the same way as above, that the most important change was that of the surface dipole component of the metal work function [20]. In these explanations it is assumed that chemical reactions the same as those at the metal–gas interface occur even at the metal–semiconductor interface, changing the barrier heights. The above experimental results may be explained using the present model without this assumption.

Acknowledgments

The authors wish to express their thanks to Professor A. Yoshimori of Osaka University for helpful discussions, and to Akashi Seisakusho Ltd. for kindly taking scanning electron micrographs of several metal-coated semiconductor wafers.

References

1 Y. Nakato, T. Ohnishi and H. Tsubomura, *Chem. Lett.*, (1975) 883.
2 Y. Nakato, K. Abe and H. Tsubomura, *Ber. Bunsenges. Phys. Chem.*, *80* (1976) 1002.
3 Y. Nakato, S. Tonomura and H. Tsubomura, *Ber. Bunsenges. Phys. Chem.*, *80* (1976) 1289.
4 S. Menezes, A. Heller and B. Miller, *J. Electrochem. Soc.*, *127* (1980) 1268.
5 K. W. Frese, Jr., M. J. Madou and S. R. Morrison, *J. Electrochem. Soc.*, *128* (1981) 1939.
6 W. Kautek, J. Gobrecht and H. Gerischer, *Ber. Bunsenges. Phys. Chem.*, *84* (1980) 1034.
7 R. N. Dominey, N. S. Lewis, J. A. Bruce, D. C. Bookbinder and M. S. Wrighton, *J. Am. Chem. Soc.*, *104* (1982) 467.
8 A. Heller, E. Aharon-Shalom, W. A. Bonner and B. Miller, *J. Am. Chem. Soc.*, *104* (1982) 6942.
9 M. Szklarczyk and J. O'M. Bockris, *J. Phys. Chem.*, *88* (1984) 1808.
10 A. J. Bard, *J. Photochem.*, *10* (1979) 59.
11 T. Kawai and T. Sakata, *Nature (London)*, *282* (1979) 283.
12 M. Matsumura, Y. Saho and H. Tsubomura, *J. Phys. Chem.*, *87* (1983) 3807.
13 M. Graetzel (ed.), *Energy Resources Through Photochemistry and Catalysis*, Academic Press, New York, 1983.
14 Y. Nakato, M. Yoshimura, M. Hiramoto, A. Tsumura, T. Murahashi and H. Tsubomura, *Bull. Chem. Soc. Jpn.*, *57* (1984) 355.
15 Y. Nakato, Y. Egi, M. Hiramoto and H. Tsubomura, *J. Phys. Chem.*, *88* (1984) 4218.
16 Y. Nakato, M. Hiramoto, Y. Iwakabe and H. Tsubomura, *J. Electrochem. Soc.*, *132* (1985) 330.
17 Y. Nakato and H. Tsubomura, *Isr. J. Chem.*, *22* (1982) 180.
18 Y. Nakato, M. Shioji and H. Tsubomura, *Chem. Phys. Lett.*, *90* (1982) 453.
19 N. Yamamoto, S. Tonomura, T. Matsuoka and H. Tsubomura, *Surf. Sci.*, *92* (1980) 400; *J. Appl. Phys.*, *52* (1981) 6227.
20 D. E. Aspnes and A. Heller, *J. Phys. Chem.*, *87* (1983) 4919.